CM.

N 341 72—06

PAPERS PRESENTED BY JAPAN
AT THE MEETING ON VOID COEFFICIENT
OF HEAVY WATE RMODERATED BOILING
LIGHT WATER COOLED REACTORS, PARIS.
18—20 SEPT. 1972

MULTIGROUP NUCLEAR COMPUTER CODE FOR CLUSTER-TYPE FUEL LATTICES: CLUSTER-IV

September, 1972

Power Reactor and Nuclear Fuel
Development Corporation, Tokyo, Japan

Multigroup Nuclear Computer Code for Cluster-type Fuel Lattices : CLUSTER-IV

September, 1972

Yoshio WATARI*
Kazuko YAMAMOTO**
Shigeru OHTERU***

The CLUSTER-IV code is a FORTRAN-4. The code is used to calculate lattice parameters for the heavy and light water moderated reactor cells containing cluster fuel elements. Solution of the transport equation is provided by a semi-analytical collision probability method. A burn-up calculation is also included, which considered twelve heavy elements, two high cross section fission products and eight pseudo fission products. The output of the code provides eigenvalue and cell average parameters for use in overall reactor calculations. Various reaction rate edits are provided for direct comparison with experimental measurements.

* Hitachi Works, Hitachi Ltd., Hitachi-shi, Ibaraki-ken

** Atomic Energy Research Laboratory, Hitachi Ltd., Ozenji Kawasaki-shi

*** Power Reactor and Nuclear Fuel Development Corporation, Tokyo

Multigroup Nuclear Computer Code for Cluster-type Fuel Lattices: CLUSTER-IV

Contents

I. Introduction

(1) The CLUSTER-IV is a general code for reactor lattice cell and burn up calculations covering a variety of reactor systems. The basic library has been compiled with 68 fast and 30 thermal groups derived from the RBU-library. The output of the code provides space dependent multigroup spectrum, four factors, multiplication factor and a few group constants for use in overall reactor calculations.

This has been programmed for HITAC-5020F and the time required for calculation is comparable with the standard multigroup calculation scheme.

(2) For the successful application of the collision probability method to multigroup calculations, a new approximation for calculating first flight collision probabilities in cluster fuel lattices is proposed based on the sub-cell model.

The unit cluster is divided into sub-regions of: fuel pins (with or without cladding) arranged in rings, associated coolant, and homogeneous annular regions surrounding the fuel region. The fuel pins and associated coolant are treated separately, and each is distinguished ringwise as a different sub-region. The collision probability is calculated between these sub-regions. The fuel annulus for containing the starting neutron is treated rigorously with consideration given to the non-uniform structure of the annulus. The other fuel annuli, on the other hand, are treated approximately as if each annulus were homogeneous. The values of the homogenized cross sections of the annuli are determined in such manner that the number of outgoing neutrons from the homogenized annuli equals that from the actual non-uniform fuel annuli.[24] The homogenized cross sections of the annuli, thus determined, are quite different from those of the volume average, in the case where a cross section included in the non-uniform annulus differs significantly from the rest of the annulus. This is the effect of the non-uniform nature of the annulus structure, and it plays an important role in such problems as resonance absorption (leading to infinitely large fuel cross section), and the treatment of air coolant. The collision probability is then apportioned among the fuel pins and the coolant in the annulus. The present method is similar to that of Bollacasa & Bonalumi,[25] but the treatment of the interaction between sub-regions in one annulus is more rigorous.

The results of the present method compare favorably with those from direct calculation by methods that are exact in principle but very time-consuming.

(3) The accuracy of the method of calculation is tested by comparing the result with experiment. The overall result has proved that the calculated values are sufficiently accurate for a variety of fuel and coolant materials.

II. Outline of theoretical model and basis

II-1. Basic Equation

Starting from the integral form of the time independent Boltzmann transport equation, the basic equation of the collision probability theory can be obtained as follows.[5]

Let $\phi(\vec{r}, E, \vec{\Omega})$ be the neutron angular flux. The integral transport equation is, then,

$$\phi(\vec{r}, E, \vec{\Omega}) = \int \frac{d\vec{r}'}{4\pi |\vec{r}-\vec{r}'|^2} e^{-\tau(\vec{r}', \vec{r}, E)} S(\vec{r}', E, \vec{\Omega}), \quad (1)$$

where $S(\vec{r}, E, \vec{\Omega})$ is the total neutron source density at the space point $\vec{r}$, at energy E and in the direction $\vec{\Omega}$. In general, $S(\vec{r}, E, \vec{\Omega})$ contains fission, scattering and external sources; $\tau(\vec{r}', \vec{r}, E)$ is the optical length between the space points $\vec{r}'$ and $\vec{r}$ for a neutron of energy E.

Consider an infinitely extended periodic lattice, and subdivide a unit lattice cell into N small sub-regions. In each of the small regions the nuclear cross section is assumed constant. Under this assumption the integral transport equation is reduced to a set of N coupled transport equations:

$$V_n \cdot \Sigma_n(E) \bar{\phi}_n(E) = \sum_{m=1}^{N} V_m P_{mn}(E) \bar{S}_m(E) \quad (n = 1, 2, \cdots, N) \quad (2)$$

where $\bar{\phi}_n(E)$ and $\bar{S}_n(E)$ are, integrated with respect to angle, the region-average neutron flux and the region-average neutron source density in sub-region n, respectively;

V_n is the volume of a small sub-region n, and $\Sigma_n(E)$ the total cross section in the sub-region n, at energy E; $P_{nm}(E)$ denotes the probability for a neutron of energy E born in a sub-region n to undergo its first collision in a sub-region m. This quantity depends on the source distribution, but for the sake of simplicity, the flat flux and isotropic scattering approximations are usually adopted:

$$P_{nm}(E) = \frac{\int_{r \in V_n} d\vec{r}\, \Sigma_n(E) \int_{r' \in V_m} d\vec{r}' \frac{1}{4\pi |\vec{r}-\vec{r}'|^2} e^{-\tau(\vec{r}', \vec{r}, E)}}{V_m} \quad (3)$$

Equation (2), together with eq. (3), are the basic equations of collision probability theory. The source density is expressed more explicitly in the form

$$S_m(E) = \chi(E) \int_0^\infty \nu \Sigma_{f_m}(E') \phi_m(E') dE'$$

$$+ \int_0^\infty \Sigma_{sm}(E' \to E) \phi_m(E') dE' + Q_m(E) \qquad (4)$$

Here, $\Sigma_{fm}(E)$ is the fission cross section in a sub-region m at energy E, and $\chi(E)$ is the distribution function of fission neutrons; $\Sigma_{sm}(E \to E')$ is the scattering kernel in a region m, and $Q_m(E)$ is the external source supplied from outside to the system under consideration. In a self-sustaining system, $Q_m(E)$ must be zero. To perform the numerical calculation, E the continuous variable of energy is changed into the discrete variable g, say group g. Equations (2) and (4) are thus reduced to:

$$V_n \Sigma_n^g \phi_n^g = \sum_{m=1}^{N} V_m P_{mn}^g S_m^g \qquad (5)$$

$$S_m^g = \chi^g \sum_{g'=1}^{G} \nu \Sigma_{fm}^{g'} \phi_m^{g'} + \sum_{g'=1}^{G} \Sigma_{sm}^{g' \to g} \phi_m^{g'} + Q_m^g \qquad (6)$$

where Σ_n^g and other cross sections are averaged, and the neutron flux ϕ_n^g is integrated over the energy interval ΔE^g belonging to group g. Collision probabilities are calculated group-wise.

II-2. Semi-analytical treatment of collision probabilities

Although Eq. (3) can be solved without any knowledge of flux, it is not so easy to obtain the numerical values of collision probabilities for lattices of complex geometry like those of cluster type fuel element. Approximations are therefore necessary. Let the clustered fuel region be subdivided into concentric annuli, numbered outwards from 1 up. Each fuel annulus contains fuel pins and associated coolant (Fig. 1). Cladding of the fuel pin is permissible. Each boundary of the fuel annulus is so chosen as to give an equal amount of coolant to each fuel pin. The fuel region is surrounded by homogeneous annular regions.

The collision probability is calculated for a neutron proceeding from one sub-region to another. The fuel annulus from which a neutron starts

is treated accurately by taking into consideration the non-uniform structure of the annulus using the sub-cell model. The other fuel annuli, however, are treated approximately as if it were homogeneous. Homogenized cross sections of the annuli are so determined that the number of outgoing neutrons from the homogenized annuli is equal to that from the actual non-uniform fuel annuli. The collision probability is then partitioned among fuel pins and coolant in the annulus. The outline of the semi-analytical method proposed for calculating collision probabilities is as follows:

We assume that all fuel pins in one annulus have the same macroscopic cross section and are located at the same distance from the center. Moreover it is assumed that they are in the same flux level. The sub-region is denoted as [i, l] or [j, k] where i or j means the annulus and l or k means fuel pin (f), fuel sheath or cladding (s), or coolant (c). The probability for a neutron born in sub-region [i, l] to undergo its first collision in sub-region [j, k] is denoted by $P_{ij}(l, k)$[4].

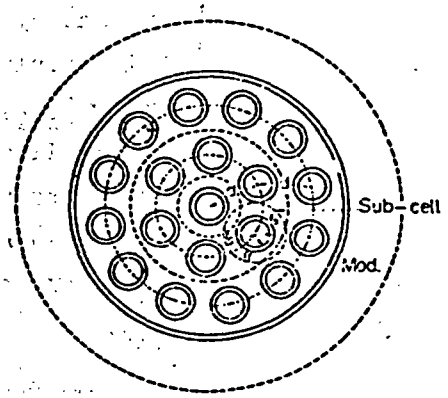

Fig. 1 19-pin cluster (circular)

(1) Diagonal Part (Fuel annulus)

Consider first the diagonal part $P_{ii}(l, k)$. By analogy with Bonalumi's P_{ii}, $P_{ii}(l, k)$ is divided into two parts, $P'_{ii}(l, k)$ and $P''_{ii}(l, k)$.

$$P_{ii}(1, k) = P'_{ii}(1, k) + P''_{ii}(1, k) \tag{7}$$

$$P'_{ii}(1, k) = p_{1k} + \frac{p_{1b}\gamma^{(i)}p_{bk}}{1-\gamma^{(i)}p_{bb}} \tag{8}$$

$$P''_{ii}(1, k) = Ps_{i-1}(1)(1-Ps_{i-1}in)G_{i-1,i}\alpha_k \tag{9}$$

$$Ps_{i-1}(1) = p_{1b}(1-\gamma^{(i)})\frac{1-\theta^{(i)}}{1-\gamma^{(i)}p_{bb}} \tag{10}$$

The first part $P'_{ii}(1, k)$ is the contribution from neutrons born in the sub-region $(i, 1)$ making their first collisions in the sub-region (i, k) without crossing inward than annulus i. In this paper $P'_{ii}(1, k)$ is obtained using the sub-cell model. The sub-cell is so determined as to obtain identical sub-cells composed of a fuel pin and associated coolant with Wigner-Seitz-cell boundary. The second part $P''_{ii}(1, k)$ is the contribution from neutrons entering the interior of the annulus i before undergoing their first collisions in the sub-region (i, k). In Eq. (8) p_{1k} is the intra-sub-cell collision probability from 1 to k, in particular, b means sub-cell boundary, $\gamma^{(i)}$ is the ratio of neutrons at the sub-cell boundary entering the next neighboring sub-cell of the same annulus, $Ps_{i-1}in$ is the probability that the neutron leaving isotropically the inner surface S_{i-1} of the annulus i undergoes the first collision in the inner region surrounded by S_{i-1}, G_{ij} is the striking probability as termed by Bonalumi. These quantities $Ps_{i-1}in$ and G_{ij} are calculated for homogenized fuel annuli using Bonalumi's method. Here, $\theta^{(i)}$ is the ratio of outgoing neutrons leaving the annulus i through its outer surface S_i and is given by $S_i/(S_i+S_{i-1})$. The apportionment of collision probability is given by $\alpha_k = p_{bk}/(1-p_{bb})$.

The homogenized cross section of each fuel annulus is determined by letting the number of neutrons leaving the homogenized annulus equal that leaving the actual, heterogeneous one. This condition is expressed by the formula

$$\Sigma^{(i)}_{homo} V^{(i)}(1-P'_{ii}) = \frac{\sum_1 \{(\Sigma V)^{(i1)} p_{1b}\}(1-\gamma^{(i)})}{1-\gamma^{(i)}p_{bb}} \tag{11}$$

where Vs are the volumes of corresponding regions. This equation has two unknowns, $\Sigma^{(i)}_{homo}$ and $\gamma^{(i)}$, but when all cross sections are equal to, say Σ, the homogeneous cross section must be Σ. Then,

$$\gamma^{(i)} = \frac{(1-P_c(\Sigma r_c))-(1-P'_{ii})}{(1-P_c(\Sigma r_c))-P_{bb}(1-P'_{ii})} \qquad (12)$$

where r_c is the sub-cell radius. The value of $\gamma^{(i)}$, as can be seen from Eq. (12), depends on the geometry and the cross section. We here assume that $\gamma^{(i)}$ can be obtained from Eq. (12) using the volume averaged cross section Σ of the annulus, even if the cross sections in the fuel annulus are not uniform. Numerical trials show that $\gamma^{(i)}$ is not very sensitive to Σ (see Fig. 2).

The effective homogeneous cross section $\Sigma^{(i)}_{homo}$ of annulus i is then determined from Eq. (11).

As an example, Fig. 2 shows the result of calculations based on Eq. (11) for a 19-pin cluster lattice. The homogenized cross section obtained here (solid line) approaches a finite value with increasing fuel

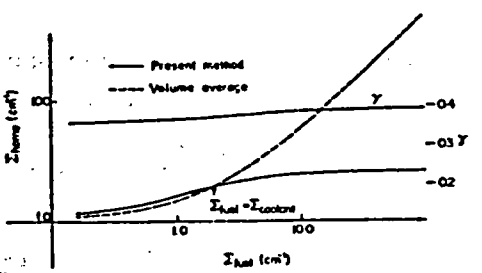

Fig. 2 Homogenized cross section in second annulus

cross section, while the volume-averaged cross section increases to infinity (dotted line). This means that even if the fuel cross section tends to infinity, a finite number of neutrons passes through the fuel annulus (because of the localized effect of fuel pins). The limiting value of $\Sigma^{(i)}_{homo}$ is determined from the dimensions of the fuel pin, of the annulus etc. and from the cross sections of the material surrounding the fuel pins (coolant etc.).

(2) Off Diagonal Part ($i < j$)

If j is a fuel annulus;

$$P_{ij}(1, k) = P'_{ij}(1, k) + P''_{ij}(1, k), \qquad (13)$$

$$P'_{ij}(1, k) = P_{is_{i-1}}{}^{(1)}(1 - P_{s_{i-1}in})\, G_{i-1j}\, \alpha_k, \qquad (14)$$

$$P''_{ij}(1, k) = P_{is_i}{}^{(1)}\, G_{ij}\, \alpha_k, \qquad (15)$$

$$P_{is_i}(1) = P_{1b}(1 - \gamma^{(1)}) \frac{\theta^{(1)}}{1 - \gamma^{(1)} P_{bb}} \qquad (16)$$

where $P''_{ij}(1, k)$ and $P'''_{ij}(1, k)$ are respectively the parts of $P_{ij}(1, k)$ that do and do not penetrate inwards from the annulus i before undergoing collision in the sub-region k of the annulus j.

If j is an outer non-fuel annulus, α_k must be equal to 1. Moreover if i also is a non-fuel annulus, $P_{ij}(1, k)$ becomes simply P_{ij}, which is none other than Bonalumi's collision probability for an annular system. Collision probabilities for $i > j$ can be calculated from reciprocal relationship.

The collision probabilities should satisfy the conservation condition. In the present case it means

$$\underset{kj}{SS}\, P_{ij}(1, k) = 1, \qquad \text{(for all (i, 1))} \qquad (17)$$

or

$$P_{is_{i-1}}{}^{(1)} P_{s_{i-1}in} = \underset{K}{S} \sum_{j=1}^{i-1} P_{ij}(1, k) \quad (\text{for } i \geq 2). \qquad (18)$$

Here, however, this relation holds only approximately*, since the neutron path from (i, 1) terminates at the surface S_{i-1}, beyond which isotropic inward penetration is assumed. We therefore normalize the collision probabilities, beginning with $P_{1j}(f, k)$, so that Eq. (17) is satisfied in addition to the reciprocity theorem.

Lattice effect is taken into account by assuming isotropic reflection at the outermost boundary B of the homogeneous annuli:

$$\bar{P}_{ij}(l, k) = P_{ij}(l, k) + \frac{P_{iB}(l, \,)\, P_{Bj}(\,, k)}{1 - P_{BB}} \qquad (19)$$

A detailed description of this method is found in the reference paper (4).

---

* The numerical results show that the summation of the left-hand side of Eq. (17) carries an error of 3 % at most.

II-3. Multigroup Calculation Scheme

In the method presented here, the 69-energy group scheme is adopted. The group constants for this scheme are assumed to be independent of the weighting spectra used to generate them, except the thermal group (the 69-th group of the scheme) constants and the resonance cross sections. These are calculated space-point-wise for each case prior to the 69-group calculation, using the same type of equations as Eqs. (5) and (6) in each restricted energy interval.[6] [9]

In order to obtain the weighting spectra for effective thermal group constants, Eq. (5) is solved in the energy region below E_l with fundamental library data of 30 groups.[6] The upper boundary E_l of the weighting thermal spectrum must be chosen sufficiently large enough so that only few neutrons scatter up across E_l. The first term of Eq. (6) is set to zero, and Q_n^g represents the source of epithermal neutrons above E_l. The scattering kernel in this case is the thermalization kernel. Group constants are obtained by energy integration within the thermal energy region between 0 and E_c ($E_c < E_l$). The thermal cut-off energy, E_c is given as input data.

For the resonance absorption of heavy nuclei contained in the fuel, the flux varies so rapidly even in one group that effective cross sections must be obtained by including more detailed information on the flux within a resonance level. For this purpose, Eq. (5) is solved for each resonance level[7],[8] with much finer energy intervals, where g is to be read as energy mesh instead of group.

The following assumptions are adopted:

(1) Resonance levels are treated separately

(2) The neutron flux has an asymptotic form (1/E) at the top energy of each resonance level.

(3) Resonance absorbers and moderating nuclei in the fuel are treated with narrow or wide resonance approximations, or purely numerically, according to the character of the resonance level, but other nuclei outside the fuel are all treated with narrow resonance approximation.

With the resonance flux thus obtained, the effective cross sections of group g of the 69-group scheme become

$$\sigma_{xi}^{g,l} = \sum_{E \in g} \sigma_x^g(E)\,\phi_i^l(E) \Big/ \sum_{E \in g} \phi_i^l(E) , \qquad (20)$$

where l and i denote resonance level and space point respectively, and x is fission or absorption, while E means energy mesh. The statistical model is used for the unresolved resonance region and the effect of the cluster is considered in the form of Dancoff factor which is calculated from P_{nm}.

The neutron leakage effect on the spectrum is included under the assumptions of fundamental buckling mode B and of diffusion approximation. The absorption cross section Σ_{ai} of the region i is replaced by $\Sigma_{ai} + DB^2$. The diffusion constant D of the lattice, while it will be finally obtained by the Benoist method, is obtained provisionally from the volume average in the lattice. The neutron flux distribution over the whole energy range in a lattice of cluster geometry is obtained by solving Eq. (5) with effective thermal and resonance cross sections and the other 66-group data.

Neutron scattering is, in practice, not isotropic and a convenient way of taking this into account in neutron transport calculation is to use the transport approximation. In the thermal energy region, the following form of transport approximation is recommended by Honeck:[10]

$$\Sigma_s^{g \to g'} = \Sigma_{so}^{g \to g'} - \delta_{g g'} \Sigma_{s1}^{g} , \qquad (21)$$

$$\Sigma_{s1}^{g} = \sum_{g'} \Sigma_{s1}^{g \to g'} , \qquad (22)$$

where $\delta_{gg'}$ is the Kronecker delta function, and $\Sigma_{so}^{g \to g'}$ and $\Sigma_{s1}^{g \to g'}$ are isotropic and anisotropic parts of the scattering kernel, respectively. In the present work, Eq. (22) is used for all transport equations.

II-4. Burn up calculation

Element changes in the process of burn up are shown in Fig. 3. In CLUSTER-IV the following approximations are used:

① The process described by the dotted line is neglected

② Fission products, except Xe^{135} and Sm^{149} are treated as eight psuedo isotopes (four of them come from U^{235} fission and its isotopes and the other four from Pu^{239} fission and its isotopes).

The following equation is solved ringwise in one lattice under the above approximations:

<u>for fissile and fertile elements</u>:

$$\frac{dNi}{d\tau} = -\lambda^{i} Ni + \lambda^{i-1} Ni-1 \qquad (23)$$

$$\lambda^{i} = \int \sigma_{a}^{i} \phi \, dE + \lambda_{\beta}^{i}$$

λ_{β} : Constant of β – decay

Here the suffix denoted fuel rings are left out.

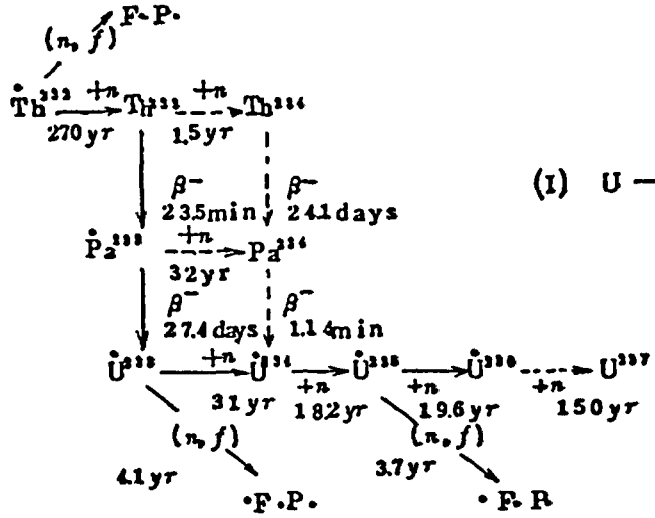

(I) U —Th^{232} Nuclide Chain

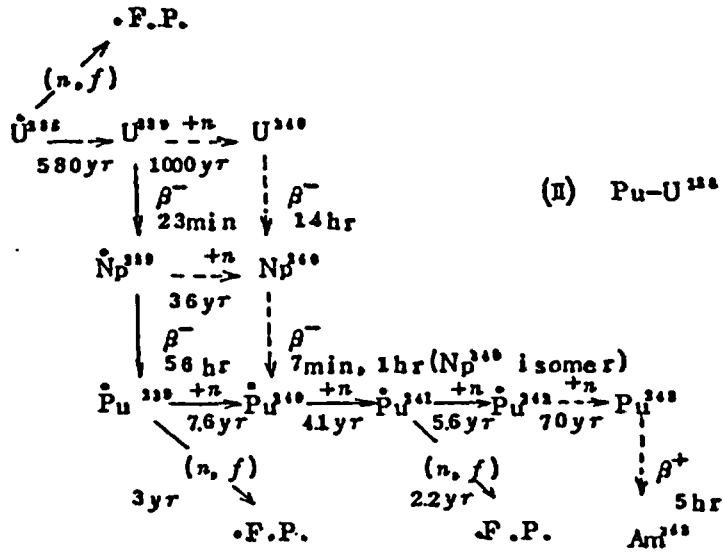

(II) $Pu-U^{238}$ Nuclide Chain

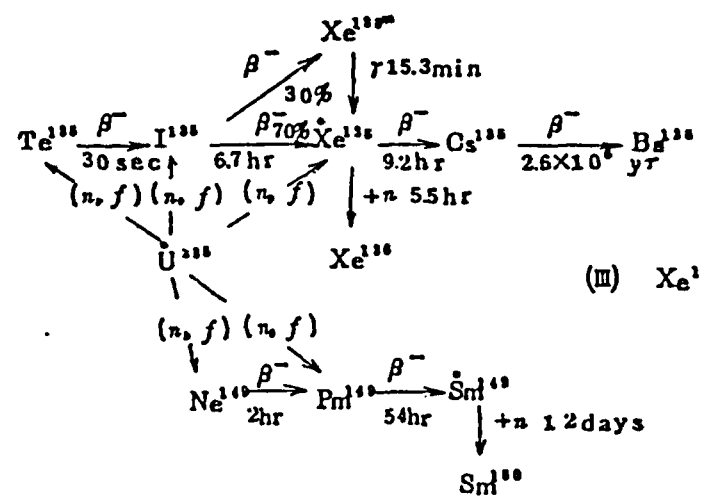

(III) Xe^{135}, Sm^{149} Nuclide Ch

Fig 3 Nuclide Chain for burnup calculation

(Burn up calculation is for the elements marked)

for fission products other than Xe^{135} and Sm^{149}

$$\frac{dN_{FP-G}}{dt} = \sum_i \left(\int y_{FP-G} \, \sigma_f^i \, \phi \, dE \right) N_i - \int \sigma_a^{FP-G} \, \phi \, dE \cdot N_{FP-G} \qquad (24)$$

$(G = 1 \sim 8)$ (where y means yield)

for Xe^{135} and Sm^{149}

$$\frac{dI}{dt} = \sum_i \left(\int y_I^i \, \sigma_f^i \, \phi \, dE \right) \cdot N_i = \lambda_\beta^I \cdot I \qquad (25)$$

$$\frac{dX}{dt} = \sum_i \left(\int y_{Xe}^i \, \sigma_f^i \, \phi \, dE \right) \cdot N_i + \lambda_\beta^I \cdot I - \left(\int \sigma_a^{Xe} \, \phi \, dE \right) \cdot X \qquad (26)$$

Where Y_I^i is summation of the yields of Te^{135} and I^{135}.

The equation for Sm^{149} are analogous to Xe^{135}.

The flux level is normalized so as to produce the power level (input).

The integration of burn up equation is done every time step (input) and element number densities changes are obtained and with which macro cross sections and multiplication factor are recalculated. Spectrum recalculation can be done under the control of input data.

Burn up is completed under the several conditions which given as input data.

An example of burn up calculation is shown in Fig. 4.

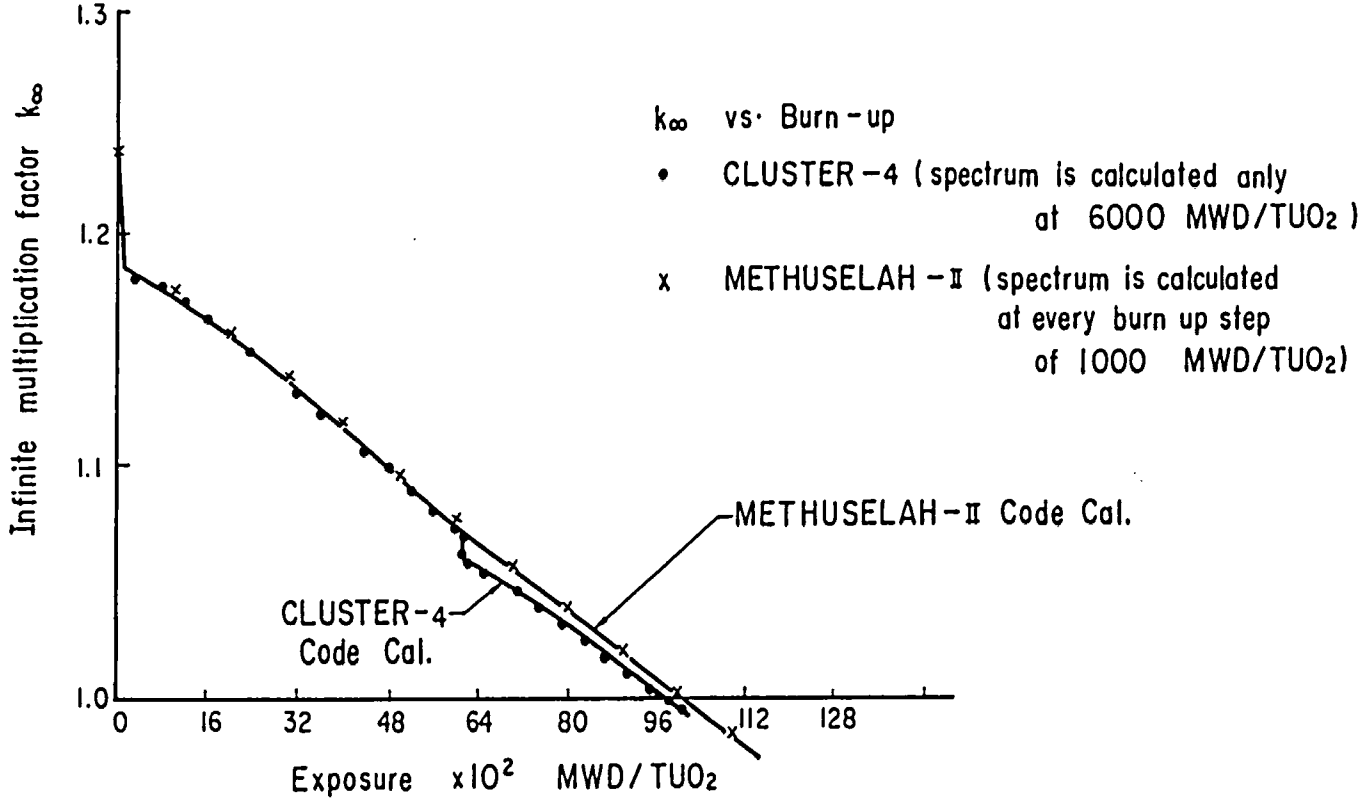

Fig. 4 Burn up behavior of k_∞ for fugen intial core.

III. Description of the code

III-1. Block chart of CLUSTER-IV

Block chart of CLUSTER-IV is shown in Fig. 5. Main parts of calculation are PAC, THERCLE, EFSLEE and BURNUP (details of which, see Sec. II). These parts are connected with the method of a code system. Fundamental data are prepared in tape and necessary data of to each calculation are selected and stored in drum. The last block of the chart, CUTPUT calculates energy and/or space integration and/or average of various quantities, such as a few group cross section, four factors, multiplication factor, effective micro cross sections, micro parameter if necessary, and so on.

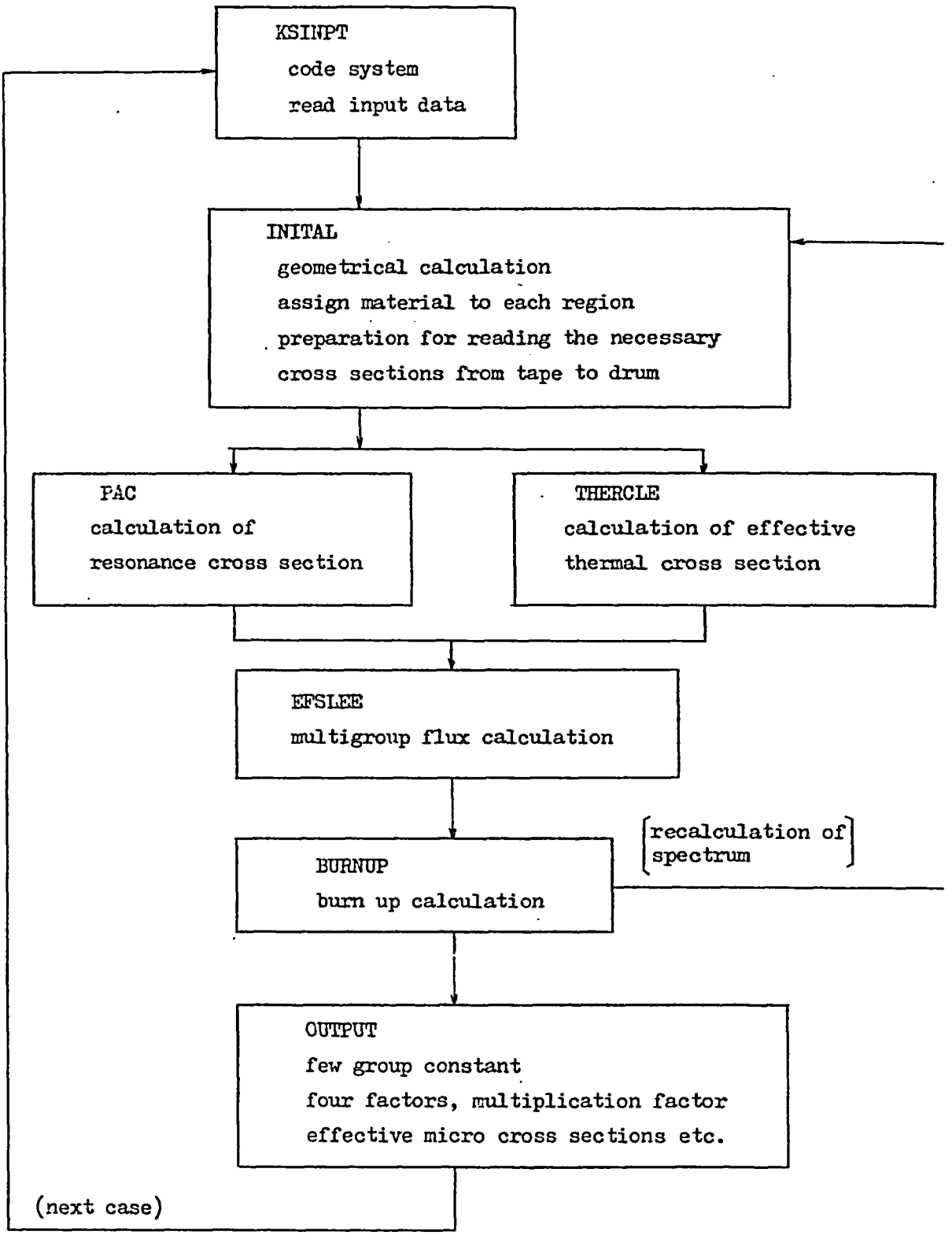

Fig. 5 Block chart of CLUSTER-IV

III-2. Library

In the library the following data are contained:

1. level parameters for resonance absorptions
2. 30 group thermal cross sections
3. 68 group cross sections for up-thermal energy region.

All these fundamental data used here derive from the RbU-library.

III-3. Limitation of calculation

1. number of region of sub-cell (= NSR) ≤ 5
2. total mesh points in sub-cell ≤ 25
3. number of fuel ring (= IRIG) ≤ 7
4. number of annular region surrounding the fuel regions ≤ 10
5. total mesh points in annular regions $\leq 25-\alpha$
   α = NSR x IRIG
6. total number of mixture ≤ 20
7. total number of isotope used in one case ≤ 50

III-4. Edit

1. resonance integral
2. effective resonance cross-section for multigroup
3. space dependent thermal spectrum
4. space dependent multi-group spectrum
5. few group constants
6. effective micro cross-section
7. four factors, multiplication factor
8. micro parameters (option)

III-5. Calculation time

Using the computer HITAC-5020F, computing time is about 15 min. for UO_2 fueled lattices (no burnup), but about 25 min. for PuO_2+UO_2 fueled lattices (depending on calculation time in PAC), as typical examples.

IV. Test of the accuracy of the code

IV-1. Collision probabilities (comparison with direct numerical calculations)

In order to test the accuracy of the method outlined in section II-2, the collision probabilities in clusters are calculated and compared with the results of Fukai and Amyot-Benoist's exact numerical methods.

First, the collision probabilities in 7-pin clusters[26] with and without cladding are calculated. The results are shown in Tables 1 and 2.

Table 1 Collision probabilities in a 7-pin cluster, (I)

$$\begin{cases} r_f = 0.6 \text{ cm} & \Sigma_f = 2.63 \text{ cm}^{-1} \\ r_s = 0.8 \text{ cm} & \Sigma_s = 0.83 \text{ cm}^{-1} \\ \text{Pitch} = 3.809 \text{ cm} & \Sigma_c = 1.52 \text{ cm}^{-1} \end{cases}$$

Collision probability from (i,l) to (j,k)	Exact[26]	Present method
$(1,f) \rightarrow$ sheath	0.06333	0.06469
$(1,f) \rightarrow$ coolant	0.22509	0.22407
$(2,f) \rightarrow$ sheath	0.06315	0.06457
$(2,f) \rightarrow$ coolant	0.22576	0.22346
$(1,s) \rightarrow$ coolant	0.51107	0.52593
$(2,s) \rightarrow$ coolant	0.51217	0.52661

Table 2 Collision probabilities in a 7-pin cluster, (II)

$$\begin{cases} r_f = 1.0 \text{ cm} & \Sigma_f = 0.1 \text{ cm}^{-1} \\ r_s = r_f & \Sigma_c = 0.66667 \text{ cm}^{-1} \\ \text{Pitch} = 3.809 \text{ cm} \end{cases}$$

Collision probability from [i,l] to [j,k]	Exact[26]	Present method
[1,f] → [1,f]	0.11498	0.11498
[1,f] → [2,f]	0.01359	0.01387
[1,f] → coolant	0.87126	0.87115
[2,f] → [2,f]	0.12007	0.12063
[2,f] → coolant	0.87764	0.87705

In Table 1, the results of "Exact" and those of the present method do not differ by more than two points in the third decimal, excepting the collision probabilities from cladding to coolant, where our method gives 3 % higher values (relative to Fukai's method*). Table 2 gives even more satisfactory results.

Fuel escape probabilities and Dancoff coefficients in hexagonal 19-pin clusters are given in Table 3. In our method the hexagonal arrangement is approximated by a circular one. All the values from our method agree within 1 %.

* Fukai's method gives accurate collision probabilities for cases without cladding, but the accuracy drops by about 1 decade if there is cladding.[27]

Table 3 Comparison of escape probabilities P_{es} and Dancoff correction factor 1-C in a hexagonal 19-pin cluster (Pitch/r_f = 2.6935)

	$\Sigma_f r_f$	$\Sigma_c r_f$ = 0.5		$\Sigma_c r_f$ = 1.0		$\Sigma_c r_f$ = 2.0	
		Exact[28]	Present method	Exact[28]	Present method	Exact[28]	Present method
P_{es}	0.1	0.8214	0.8177	0.8541	0.8539	0.8752	0.8762
	0.25	0.6434	0.6396	0.6977	0.6988	0.7348	0.7373
	0.5	0.4659	0.4644	0.5278	0.5306	0.5727	0.5764
	1.0	0.2923	0.2926	0.3448	0.3485	0.3853	0.3892
	2.0	0.1617	0.1623	0.1952	0.1977	0.2218	0.2244
	5.0	0.0669	0.0670	0.0814	0.0823	0.0930	0.0939
1-C	100.0	0.6732	0.6740	0.8196	0.8276	0.9367	0.9460

$$P_{es} = 1 - \frac{1}{\sum_i m_i} \{ \sum_i m_i P_{ij} (f, f) \}, \qquad 1 - C = \lim_{\Sigma_f \to \infty} \{ 2 \Sigma_f r_f P_{es} \}$$

m_i Number of fuel pins in i-th annulus

Figures 6 to 8 show fuel to fuel collision probabilities in circular 19-pin clusters with air coolant[26] (see Fig. 1, but ignore cladding). The present method gives values a little higher than exact for collision probabilities between fuels in the same annulus, $P_{22}(f,f)$ or $P_{33}(f,f)$, but lower values for inter-annular collision probabilities $P_{23}(f,f)$, especially when the pin-pitch is narrow.

For cases with air coolant the treatment based on the sub-cell model may become less accurate, and the error introduced by terminating the neutron path at the boundary of an annulus may be accentuated. Moreover the pin arrangements used here are not quite the same as those adopted in the "Exact" method, because in our method the pin-pitch d is not an input data as in the other method. This should add to the deviation of the collision probabilities from the exact values. However the errors are still within 5 %.

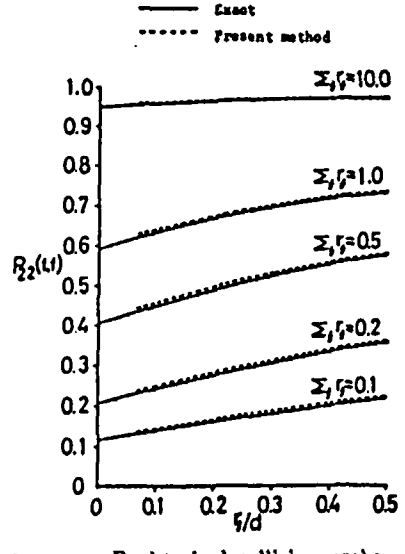

Fig. 6 Fuel-to-fuel collision probability in second annulus of 19-pin cluster of type shown in Fig. 1 (without cladding)

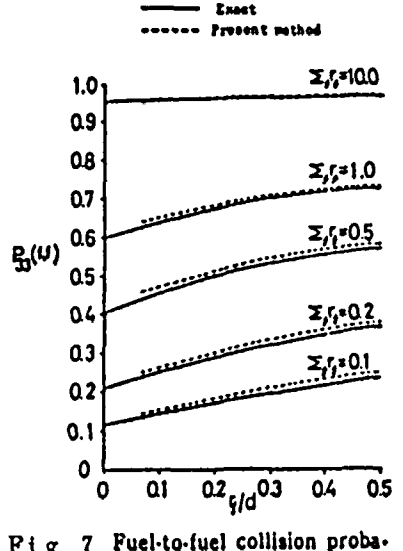

Fig. 7 Fuel-to-fuel collision probability in third annulus of 19-pin cluster of type shown in Fig. 1 (without cladding)

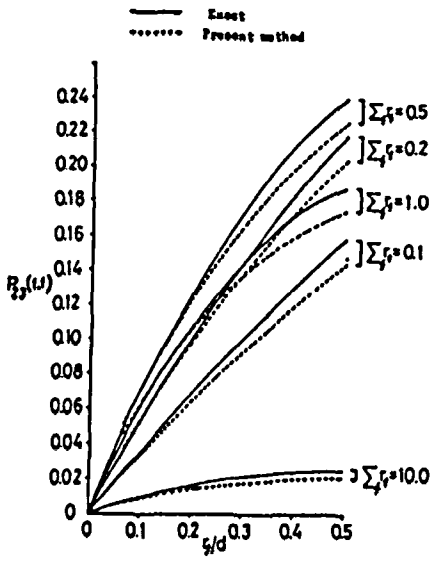

Fig. 8 Collision probability in fuel of third annulus for neutron born in fuel of second annulus (without cladding)

IV-2. Resonance integral

The values of the calculated resonance integrals for infinite dilution are compared in Table 4 with those of the experiment. This shows that the fundamental data used in the calculations are consistent with the experiment.

By using the transport approximation, anisotropic scattering effect of neutron transport calculation is considered in chapter II-3. To justify the validity of this procedure, a comparison with the experiment on resonance is shown in Table 5. The resonance integrals in Table 5 (Cal. 2) are in satisfactory agreement with the experimental results under the condition of narrow resonance approximation in moderator.

Table 4 Resonance Integral (RI^{∞} barn)

Isotope	Re-action	Resonance Integral		Higher	1/v (0.5)	R I	
		Resolved	Un-resolved			CLUSTER-III	Exp. (BNL-325)
U^{235}	f	92.2	112.7	17.9	40.3	263.1	274 ± 10
U^{238}	c	272.2	2.0	2.7	1.2	278.1	280 ± 12
Pu^{239}	f	136.1	80.2	21.1	97.8	335.2	335 ± 15
Pu^{240}	c	8378.0	50.9	0.4	9.3	8438.6	8280*
Pu^{241}	f	254.0	165.4	20.2	75.8	515.4	537 ± 27

* M.K. Drake; Nucleonics (1966)

Table 5 Experimental and calculated values of U^{238} resonance integral for 19-pin clusters

Coolant / Position	H_2O			D_2O			Air		
	Exp.[19]	Cal. 1	Cal. 2	Exp.[19]	Cal. 1	Cal. 2	Exp.[19]	Cal. 1	Cal. 2
1f	12.94	15.35	13.71	10.75	12.48	12.18	9.59	10.78	10.78
2f	13.12	15.44	13.92	11.11	12.77	12.55	10.20	11.18	11.18
3f	13.93	16.66	15.31	13.43	14.90	14.50	12.53	13.63	13.63
3f'	14.41			14.20			13.91		
Av.	13.8±0.3	16.21	14.81	12.8±0.3	15.30	13.80	12.1±0.3	12.71	12.71

Cal. 1: isotropic scattering only

Cal. 2: includes anisotropic scattering approximately with transport correction

IV-3. Comprehensive comparison with the experiment of 28-rod cluster fuel latticies

The accuracy of the method of calculation is tested by comparing the results of calculation with the experiment. The calculation gived detailed information on neutron flux in space and energy. The experiment, on the other hand, gives energy integrated quantities, the energy region being separated at most into two. If the theory correctly predicts neutron flux spectra, then the integrated or averaged quantities of neutron flux spectra should be correct. The converse of this statment is not true since the agreement of averaged properties does not necessarily imply the correctness of the detailed distribution.[12] However, comprehensive comparison of various quantities of a lattice with different dependence on energy should provide an indication of the degree of accuracy of the method of calculation.

Here the following quantities are studied:

(1) Micro-parameters of lattices

(2) Reaction distribution in space

(3) Thermal disadvantage factor

(4) Thermal spectrum index

(5) Multiplication factor, or what is known as the four factors, which is a combination of the above quantities.

The lattices studied here are four kinds of 28-pin clusters with various void ratios in light water coolant, of various lattice pitches, various kinds of fuel (UO_2 or PuO_2-UO_2) and of moderator (heavy or light water). They are located in two regioned critical cores with surrounding driver region. Measurements are performed in the central unit lattice of each cluster lattice region. The void ratios in coolant vary from 0 % void (filled with light water in coolant passage) to 100 % void (filled with air coolant). Intermediate void ratios are simulated with light and heavy water mixtures. The definition of effective void ratio is not the same for D_2O-30% lattices and for H_2O-80% lattice: in the D_2O-30% lattices it means the light water volume ratio in coolant, but in the H_2O-80% lattice it denotes the effective light water density of the mixture in reference to the absorption-to-scattering rate ratio.

The spectrum is calculated under the condition that the effective multiplication factor is equal to 1.0, by seeking the self-consistent

buckling (material buckling), instead of solving the eigen-value problem with geometrical buckling.

The necessary data for the calculation are listed in Table 6.[13],[14]

Figures 10~12 show the micro parameters. The thermal cut-off energy E_c is set equal to the effective Cd cut-off energy, for which a value of 0.45 ev is used in all the lattices, considering the foil thickness used in the experiment.[15] In these figures the abscissa is the point in space where the measurement is made, for instance. If means the fuel of annulus 1 which corresponds to that of T-1 in the reference paper (22) of the present series. From the discussion in Section II-2 of the present report, the calculation assumes that positions 3f and 3f' are equivalent, although they are distinguished in the experiment.

Among the micro-parameters, δ^{28}, the ratio between the fast fission rate of U^{238} to the total fission rate of U^{235}, agrees well between measurement and calculation. Most of the calculated results are within statistical error of the experiment. Since only the first few groups in the 69-group scheme contribute to the numerator of δ^{28}, the above mentioned results show that the corresponding part of the energy is correctly calculated relative to the thermal part.

The epi-to-thermal fission ratio of U^{235} (δ^{25}) represents the epithermal neutron behavior relative to that of the thermal neutrons. Figures 10~12 show that the calculated values of δ^{25} is a little lower than that of experiment, especially for D_2O-lattices and in 100% void. The calculated value of R I^{∞} the resonance integral for U^{235} in infinite dilution, is 5% lower than by experiment (see Table 4). If this difference is corrected, the agreement becomes much better, almost within statistical error of the experiment. In the 100% voided D_2O-lattices, however, a 10% discrepancy still remains even after the correction. The calculated epi-to-thermal capture ratio of U^{238} (ρ^{28}) at 3f in 100% void for the PuO_2-D_2O lattice is about 10% lower than experiment, but there are good agreement resonance quantities δ^{25} and ρ^{28} are much more dependent on lattice pitch than is δ^{28}. This results from the fact that the moderator plays a more important role on resonance quantities. For the UO_2-H_2O lattices, the agreement of ρ^{28} is poorer, and the observed plots vary irregularly.

Lastly shown is the relative conversion ratio C^*, the ratio of the total capture rate of U^{238} to the total fission rate of U^{235} in the

lattice relative to the same ratio in the thermal column. Calculation gives a 3~15% higher value than experiment. Some discussions are given in Chapter IV-4 in this respect. In UO_2-H_2O lattices the quantity C^* has not been measured.

The micro parameters directly relate to the multiplication factor (four factors). However, for the purpose of examining the accuracy of the method, of calculation, group-wise information on the reaction rates themselves, instead of the epi-to-thermal reaction rate ratios, should be more useful. Figure 13 shows the distribution of U^{235}-fission, U^{238}-fission and U^{238}-capture rates in UO_2-D_2O lattices. The reactions in Fig. 13 are normalized so as to give the unit value for the sum of epi- and sub-Cd contribution of each reaction at the position of the fuel in the annulus 1. The figure shows that all of the calculated distribution of reaction rates in each energy group agree well with measurement. For the Pu lattices similar comparisons are given in the reference 16.

Thermal disadvantage factors are given as average Dy reaction rate ratios in the homoid region (coolant, sheath and outside homogeneous annuli such as pressure tube, calandria tube and moderator) in reference to that of the average of all the fuel pins. The results are shown in Table 7.[13],[14],[17] For D_2O-lattices the disadvantage factors of coolant to fuel in each fuel annulus are also shown. The calculated disadvantage factor tends to be a little smaller than the measured one. This tendency may arise from the treatment based on the sub-cell model. (It must be remembered that the coolant region was partitioned into annuli in portions that differ between calculation and experiment. No correction has been made in this respect).

In Table 8 the thermal spectrum index is given as Lu/Mn reaction rate ratios normalized to thermal column values. This is another important integral quantity of thermal flux showing the hardness of the thermal neutron spectrum. For UO_2 fueled lattices the calculated results are in good agreement with measured values. However for PuO_2-UO_2 fueled lattices, the calculations result in values somewhat lower than measurement in all space points and void ratio. Theoretically, the fact that the Lu/Mn reaction rate ratios are lower for PuO_2-UO_2 than for UO_2 fuel lattices is due to the large resonance of Pu^{239} at 0.3ev (see Fig. 14). However, the measured Lu/Mn reaction rate ratios in PuO_2-UO_2 fueled lattices are higher than in UO_2 fueled lattices even for those at the outer-most point of the moderator. It may suggest that the effect of the spectral disturbance from

the driver region is felt in the Lu/Mn reaction rate ratios, which are sensitive to the component of the spectrum.

The multiplication factor can be determined from the micro-parameters and disadvantage factors (see appendix). In Figure 15 comparisons are given between calculation and experiment on the fast effect ε, resonance escape probability p, thermal utilization factor f, and the multiplication factor k_∞, with various void ratios of coolant density*. For D_2O-lattices, the general tendency of the calculation to give lower values of resonance reaction than experiment, especially in the case of 100% voided lattices, results in a lower ε (owing to U^{235} fission) and in higher p (owing to U^{235} capture and U^{238} capture). For the H_2O-lattice of 0% void the calculated resonance escape probability p is 2% higher than experiment. The discrepancy results mainly from the lower value of ρ^{28} especially at 3f. The discrepancy in the thermal disadvantage factor does not so severely affect the thermal utilization factor if the system embodies heavy water moderator. For a system with light water moderator, however, the divergence more severely affects the thermal utilization and multiplication factors. The calculated multiplication factors k_∞ agree with experiment within 1%, except the cases of UO_2-D_2O-22.5 lattice of 100% void and UO_2-H_2O lattice of 0% void, although some discrepancies in ε and p are cancelled out in k_∞. The void dependence of the multiplication factor is fairly well reproduced. For UO_2-D_2O-22.5 lattice of 100% void, half of the discrepancy between calculation and experiment in k_∞ results from the disagreement in C^*. For the UO_2-H_2O lattice of 0% void, the calculated k_∞ is larger than experiment by 2%, and this is due to the lower ρ^{28}.

---

* For UO_2-H_2O lattices $C^*_{exp} = C^*_{cal}$ is assumed, and for PuO_2-D_2O lattices, moreover, $\delta^{49}/^{25}$ and δ^{49} (see appendix) are used to obtain k_∞, of which no comparison has been given in this paper (see ref. 16).

IV-4. Discussion of the results obtained in chapter IV-3

In examining the void dependence of the four factors in cluster type fuel lattices, it is seen from Fig. 15 that the miltiplication factor has a tendency to rise with increasing void fraction. This results from the fact that coolant and moderator are separated from each other and that the void occurs only in the coolant. Generally the presence of void is of advantage to the thermal utilization factor f (loss of absorber effect) but is of disadvantage to the resonance escape p (loss of slowing down effect).

In cluster lattices, neutrons are moderated mainly in the zone outside the fuel region. Even if the coolant becomes 100% void, neutrons pass into the fuel region from outside the moderator region. This results in less change of p with void in cluster than in regular lattices (a numerical trial shows that the change of p in a cluster is about one half that of a regular lattice). Since the change of p is smaller in cluster than in regular fuel lattices the repression effect is so much lower in the former type fuel lattices. Although moderation in coolant is of secondary importance in a cluster fuel lattice, it becomes more important as the moderator-to-coolant volume ratio becomes smaller (compare two UO_2-D_2O lattices with different pitch in Fig. 15).

The loss of slowing down effect also renders harder the thermal neutron spectrum in the fuel region. It reduces the advantage of f resulting from the loss of absorber effect: a numerical trial shows that the decrease of $\sigma_{a\ th}^{235}$ with void in a cluster fuel is about one half of that in a regular lattice, and that in some cases the thermal neutron spectrum in the fuel region of 100% void is softer than with other void fractions.

Comparisons between calculation and experiment have proved that the present method has a tendency to underestimate the micro-parameters the micro-parameters such as δ^{25} and p^{28}, especially when the coolant becomes voided by 100%. The calculated neutron flux spectrum corresponds to the that for a single region critical core whose configuration is the same as the test region (characteristic spectrum of the cluster lattice). On the other hand, the experimental lattices studied here are located at the center of the inner test region in two-region critical cores. Thus, in the experiment, the characteristic spectrum might be disturbed by the surrounding driver region.

A recent study[18] on the UO_2-D_2O cores indicated that the characteristic spectrum is realized in satisfactory approximation at the center of the test region if the spectrum is calculated under the assumption that the effective multiplication factor is equal to 1.0 (cf. self consistent buckling iteration method described in IV-3 above). The four-group calculation of the study gives a 3% lower ϕ_3/ϕ_4 value than the characteristic spectrum at the center of the test unit lattice of UO_2-D_2O for 100% void and almost the same ϕ_3/ϕ_4 for other void percentages (for PuO_2-D_2O lattices a little larger disturbance may occur). This could prove useful for correcting the difference between the calculated and experimental values. In this connection, we recall the experimental verification reported by Y. Hachiya and H. Hatakenaka[22]: It was there stated that in the test region the deviation of the observed spectrum from the characteristic is negligible.

Next, the Cd cut-off energy significantly affects such micro parameters as where the fast-to-thermal reaction rate considered is in small and the reaction around the Cd cut-off energy is relatively important. For example, the changes of the values of δ^{25}, ρ^{28}, δ^{28} and C^* corresponding to a change of Cd cut-off energy from 0.45ev to 0.625ev, for example, were found by calculation to be about 10%, 3%, 1% and 1%, respectively. Among these parameters, δ^{25} is the most sensitive to Cd cut-off energy.

In the experimental analysis studied here the thermal cut-off energy is equal to the Cd cut-off energy of 0.45eV. This might be considered excessively low compared with the thermal cut-off energy generally used in multigroup calculations. A theoretical verification based on a simplified shows that this value of thermal energy cut-off is still reasonable[20],[21] Moreover numerical calculation reveals that the effect of this treatment on the overall flux is small (less than 0.3% in k_∞), at least for the cases considered here.

The relative conversion ratio is expressed by

$$C_i^* = I_i \left(\frac{1+\rho^{28}}{1+\delta^{25}}\right)_i \qquad (27)$$

$$I_i = \left(C_2^{28}/F_2^{25}\right)_i / \left(C_2^{28}/F_2^{25}\right) \qquad \text{thermal column.}$$

The notations used here are found in the appendix. The change of C_2^{28}/F_2^{25} depends on the thermal spectrum, so that the remaining independent information contained in C_i^* is I_i. Generally the value of I_i is 1 for the same spectrum as that in the thermal column, and exceeds 1 for harder spectra. This holds in calculation, but not for the I_i derived from the experimentally determined values of ρ^{28}, δ^{25} and C^*. No successful explanation can be given here on this point.

The criterion of validity of the calculated flux distribution in the coolant is the thermal disadvantage factor. The calculated disadvantage factors of the coolant are lower than the experiment, especially when the coolant is not voided, and are almost same for all fuel annuli. This is the result of adopting a sub-cell model in which an equal amount of coolant is attributed to all fuel pins. This model partitions the coolant in equal amounts to all fuel pins and locates the coolant nearer to the fuel pin than in actuality. Hence, the local water peaking becomes almost the same for all fuel annuli and lower than actual, giving a smaller disadvantage factor. The lower values of the coolant disadvantage factor reduce, in turn, the tube disadvantage factor. This is the limiting factor for the validity of the semi-analytical model used here. For the multiplication factor, however, the resulting effect is small for heavy-water moderated systems.

A detailed description of the experimental methods and analysis is found in the reference literature (22), (23).

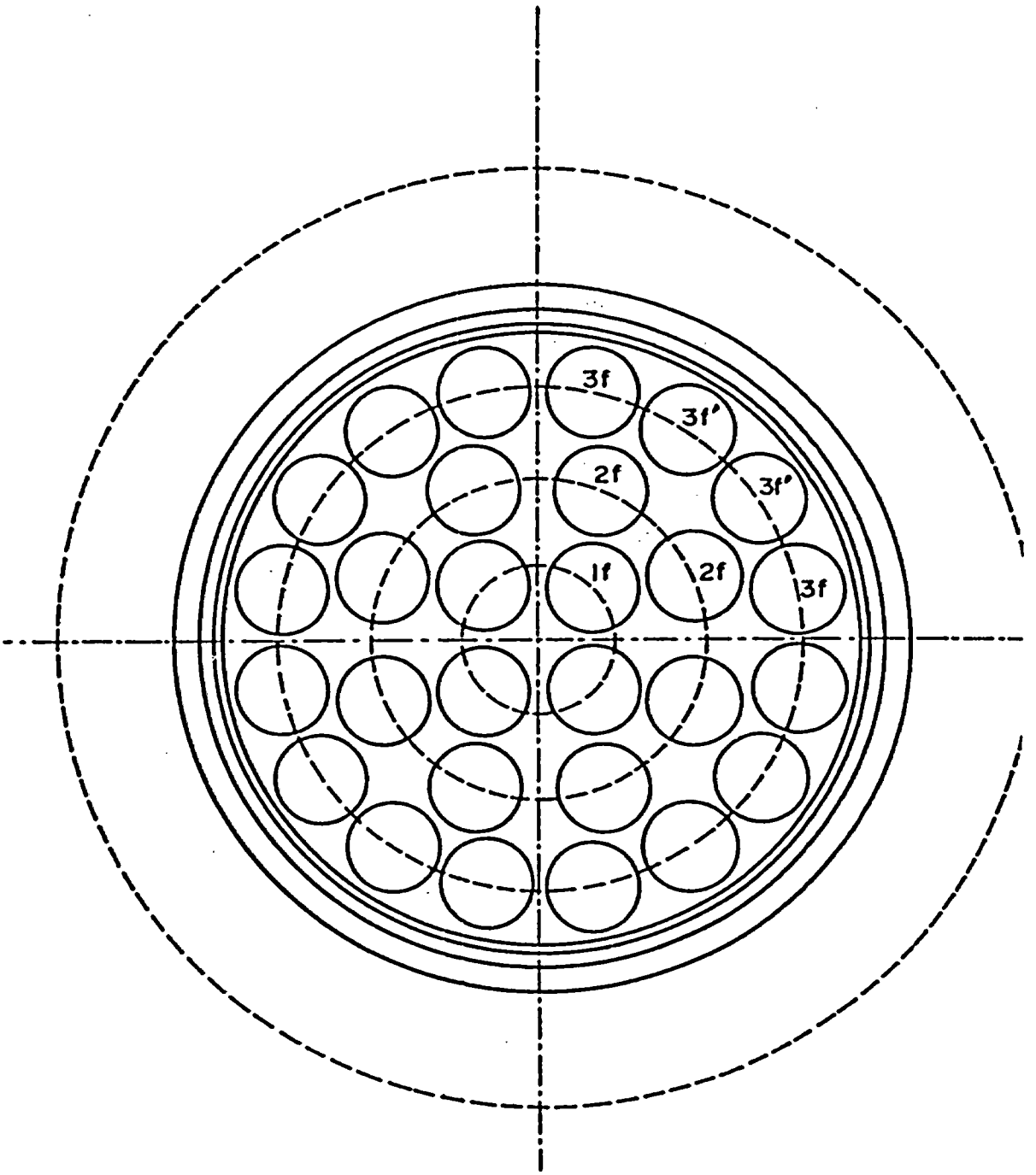

Fig. 9 Unit lattice of 28-pin cluster

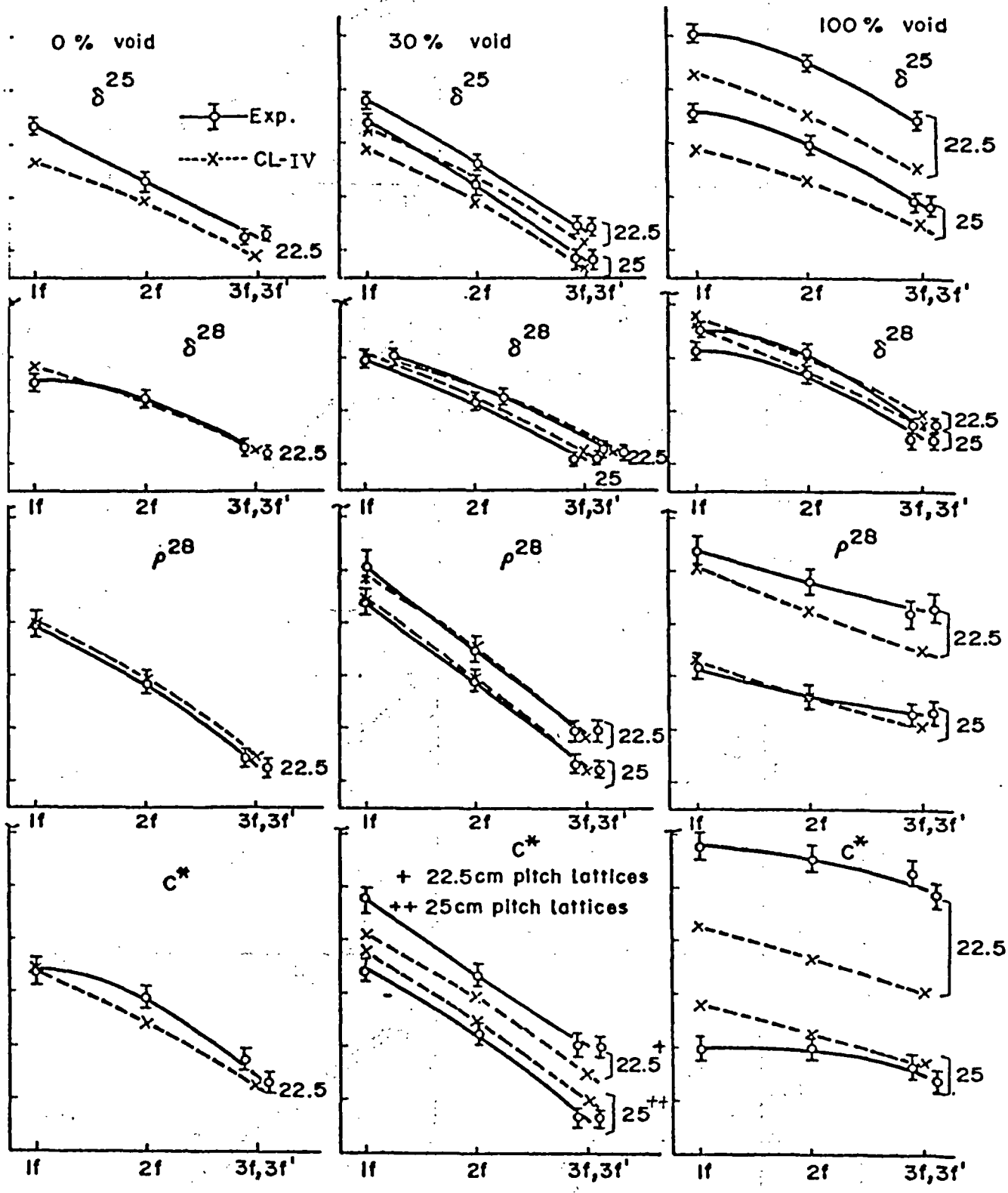

Fig. 10 Micro-parameters of UO_2-D_2O lattices

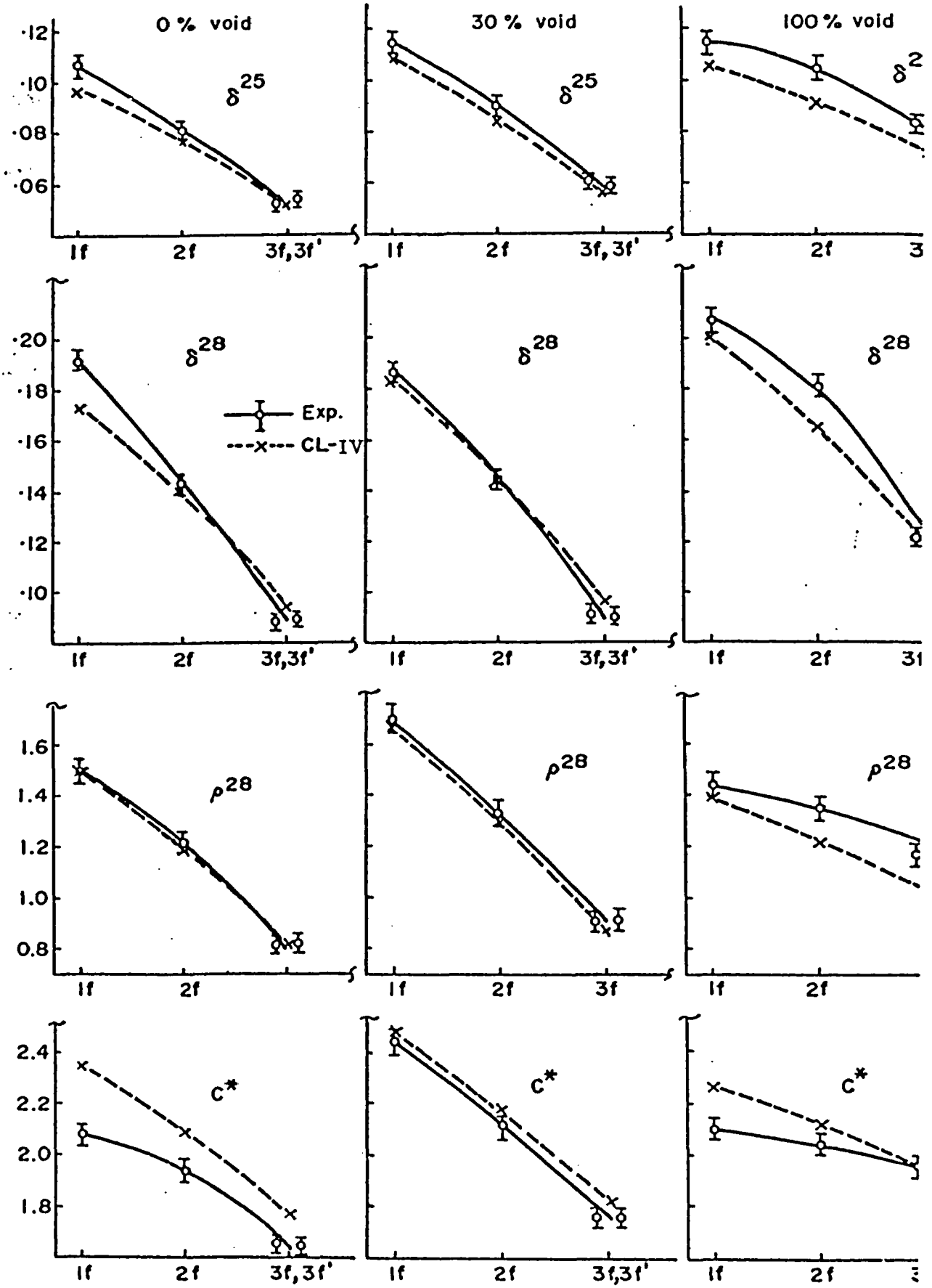

Fig. 11 Micro-parameters of PuO_2-UO_2 lattices

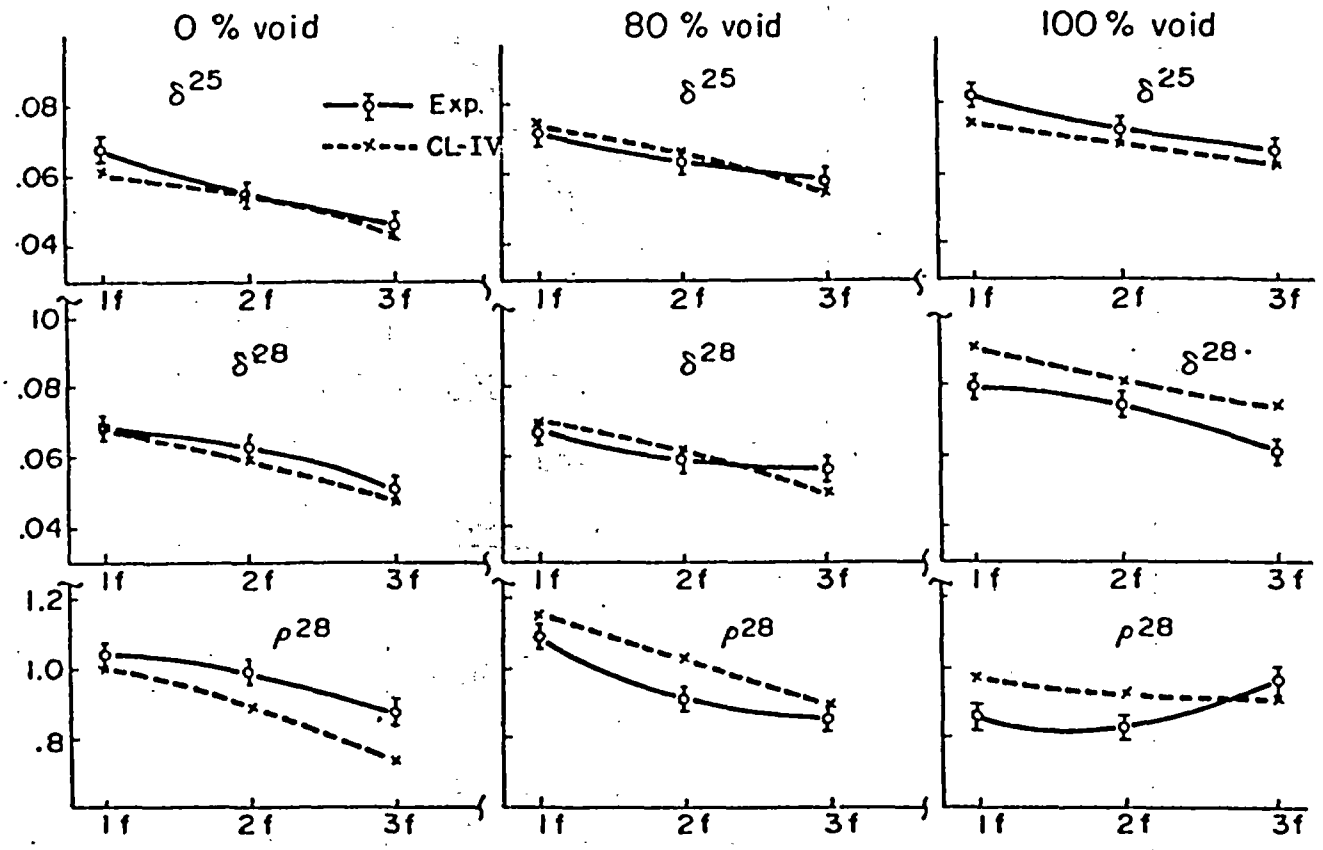

Fig. 12 Micro-parameters of UO_2-H_2O lattices

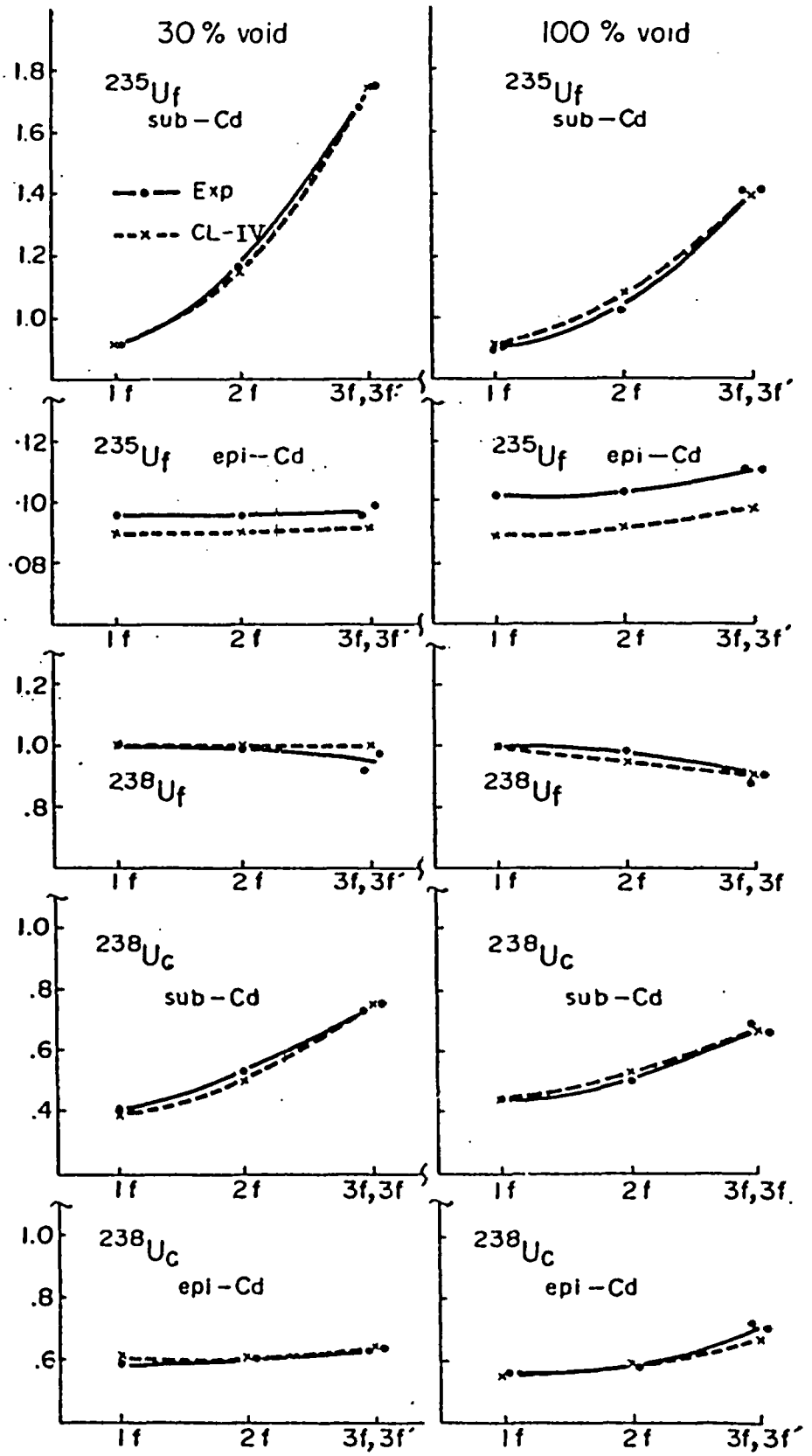

Fig. 13 Distribution of U^{235} fission, U^{238} fission and U^{238} capture (UO_2-D_2O lattices)

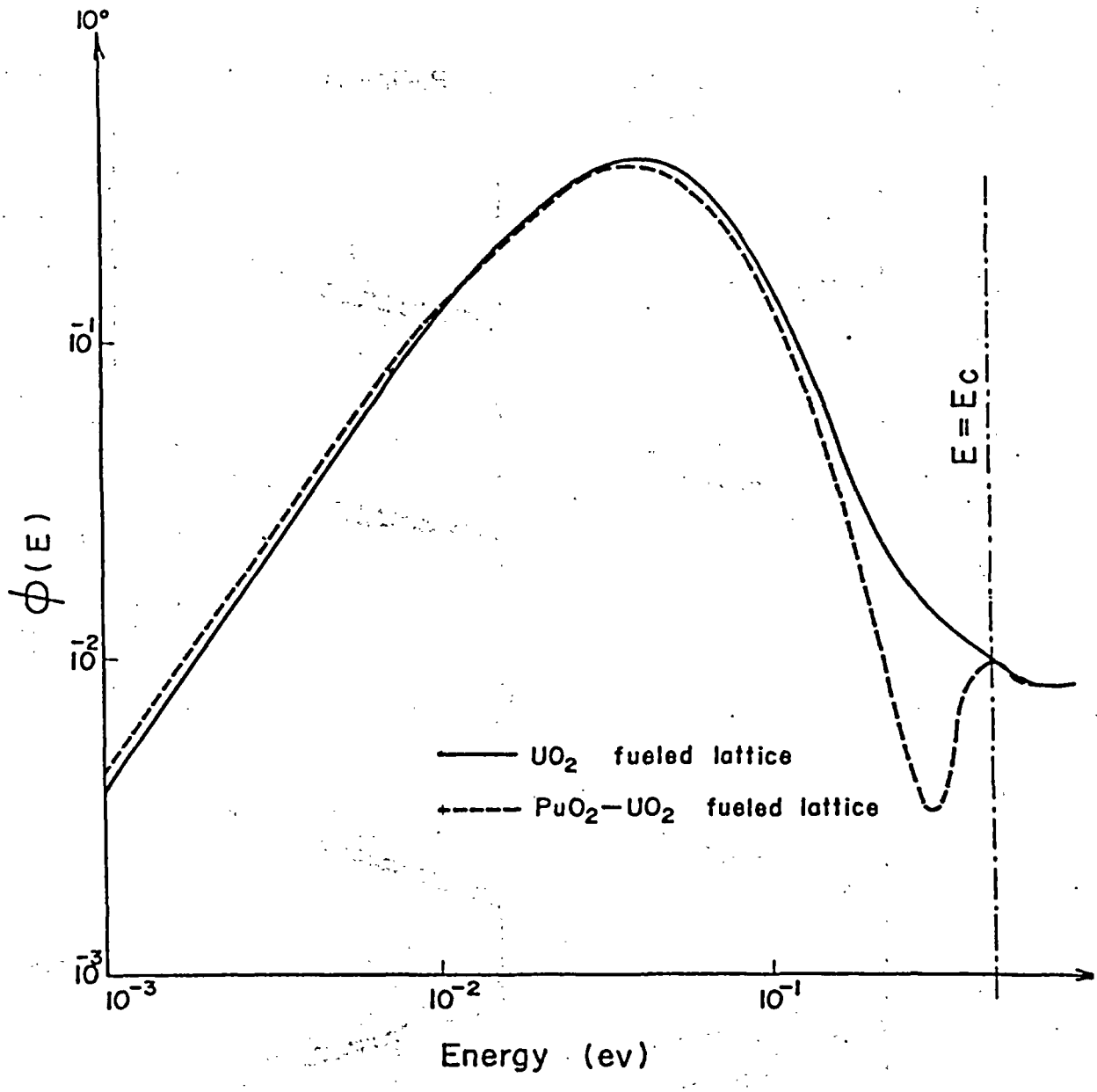

Fig. 14 Thermal neutron flux spectrum in a fuel pin at the innermost annulus of D_2O moderated 28-pin cluster lattices with 100% void coolant

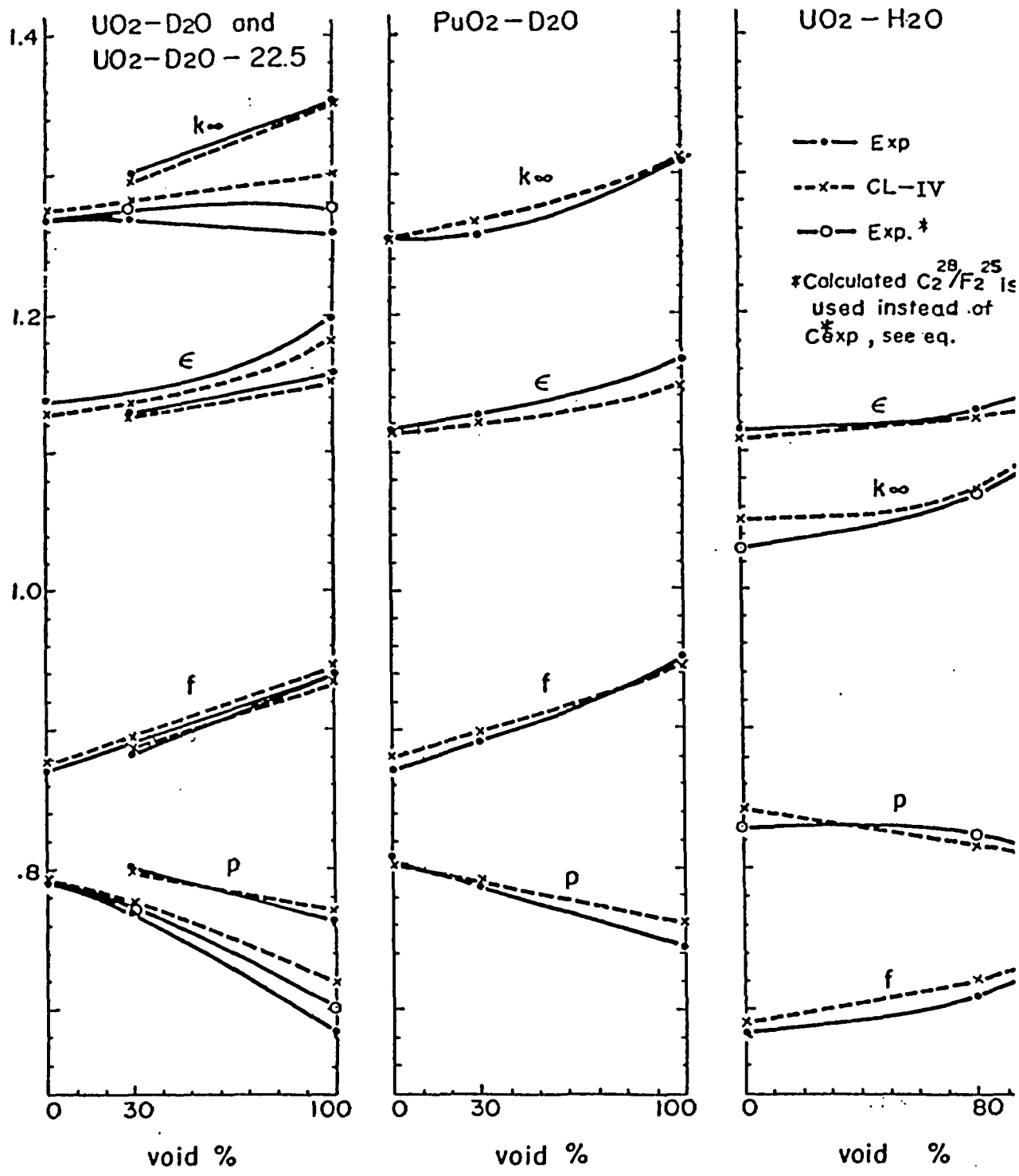

Fig. 15 The multiplication factor

Table 6 Dimensions and enrichment of lattices studied[13),(14),(17)]

Lattice	Pitch (cm)	Fuel pin					Coolant void ratio (%)	Pressure tube		Calandria tube		Moderator
		Enrich (%)		(cm)[4)]	(cm)[5)]	(cm)[6)]		(cm)	(cm)	(cm)	(cm)	(cm)
UO_2-D_2O-22.5	22.5(S)[1)]	UO_2	1.5	0.75	0.7625	0.8425	0,30,100	5.8	6.1	6.6	6.75	12.650
UO_2-D_2O	25.(S)	UO_2	1.5	0.75	0.7625	0.8425	30,100	5.8	6.1	6.6	6.75	14.105
PuO_2-D_2O	25.(S)	UO_2+ PuO_2	NU+ 0.493[3)]	0.75	0.7625	0.8425	0,30,100	5.8	6.1	6.6	6.75	14.105
UO_2-H_2O	11.2(H)[2)]	UO_2	1.5	0.5	0.57	0.61	0,80,100	4.25	4.55	-	-	5.881

1) s: square
2) h: hexagonal
3) Weight % of PuO_2 to (PuO_2+UO_2)
4) Radius of fuel pin
5) Inner radius of fuel sheath
6) Outer radius of fuel sheath

Table 7 Thermal disadvantage factor

	Lattice		UO_2-D_2O		PuO_2-D_2O			UO_2-H_2O		
	X	Void %	30	100	0	30	100	0	80	100
D.F. of region X in a unit cluster lattice	Sheath	Exp.	1.10±.03	-	1.13±.05	1.07±.05	1.03±.05	1.16	1.06	1.15
		CL-IV	1.112	1.112	1.114	1.114	1.117	1.088	1.086	1.083
	Coolant	Exp.	1.246±.034	1.109±.033	1.33±.06	1.25+.06	1.11±.05	1.23	1.25	1.11
		CL-IV	1.210	1.163	1.225	1.213	1.172	1.149	1.128	1.117
	PT	Exp.	2.18±.05	1.78±.05	2.42±.11	2.50±.11	1.70±.08	1.58	1.61	1.38
		CL-IV	2.004	1.784	2.033	2.055	1.821	1.548	1.540	1.431
	CT	Exp.	2.17±.06	1.79±.06	2.48±.11	2.55±.12	1.81±.08			
		CL-IV	2.109	1.896	2.130	2.159	1.929			
	Mod.	Exp.	2.77±.14	2.81±.14	2.96±.13	3.28±.14	2.80±.14	2.03	2.28	2.12
		CL-IV	2.837	2.818	2.867	2.961	2.934	2.001	2.132	2.089
D.F. of coolant in each ring X	1	Exp.	1.218±.025	1.404±.031	1.23±.06	1.11±.05	1.02±.05	-	-	-
		CL-IV	1.204	1.120	1.228	1.217	1.138	1.149	1.121	1.091
	2	Exp.	1.236±.021	1.108±.033	1.31±.06	1.25±.06	1.06±.05	-	-	-
		CL-IV	1.208	1.166	1.223	1.212	1.185	1.150	1.128	1.115
	3	Exp.	1.319±.041	1.187±.036	1.40±.06	1.31±.06	1.18±.05	-	-	-
		CL-IV	1.212	1.171	1.227	1.214	1.189	1.150	1.130	1.122

Table 8 Thermal spectrum index $(\sigma^{Lu}/\sigma^{Mn})_x / (\sigma^{Lu}/\sigma^{Mn})_{thermal\ column}$

Position x	Lattice Void %	UO_2-D_2O		PuO_2-D_2O			UO_2-H_2O		
		30	100	0	30	100	0	80	100
1,f	Exp.	1.38	1.57	1.45±.04	1.46±.04	1.56±.05	1.29	1.40	1.43
	CL-IV	1.396	1.570	1.317	1.339	1.459	1.309	1.428	1.462
2,f	Exp.	1.36	1.49	1.43±.04	1.38±.04	1.47±.05	1.25	1.35	1.40
	CL-IV	1.345	1.508	1.285	1.297	1.415	1.288	1.390	1.426
3,f	Exp.	1.28	1.34	1.32±.04	1.33±.04	1.42±.05	1.21	1.29	1.39
		1.28	1.35	1.37±.04	1.40±.04	1.43±.05			
	CL-IV	1.293	1.410	1.242	1.255	1.345	1.250	1.319	1.372
Mod. (outer most)	Exp.	1.05	1.15	1.10±.03	1.18±.04	1.20±.04	1.03	1.08	1.09
	CL-IV	1.104	1.133	1.098	1.104	1.130	1.095	1.108	1.119

V. Conclusion

The CLUSTER-IV code which can perform the reactor lattice-cell calculations on various reactor systems has been developed the at Atomic Energy Research Laboratory of Hitachi Ltd.

A new collision probability method is proposed and adopted in the code This treats rigorously the fuel annulus where a neutron starts, taking into consideration the non-uniform structure of the annulus. It treats, however the other annuli approximately as if it were annuli with homogeneous cross-sections. The values of these homogeneous cross-sections are determined in such manner as to allow the number of outgoing neutrons from the homogeneous annuli equal that from the actual non-uniform annuli. The method has been compared comprehensively with experiments on micro parameters, reaction distribution, thermal disadvantage factor, thermal spectrum index and multiplication factors. The studied lattices cover parameters such as fuel material, moderator material and void fraction.

The overall result has proved that the calculated values are sufficiently accurate for a variety of fuels and coolant materials, while economizing calculating time.

References

(1) Soodak, H. and Sullivan, R.: HDA2131-38 (1961)

(2) Furuhashi, A. and Yasukawa, S.: JEARI memo 1656 (1964)

(3) Aplier, R.: AEEW-R 135 (1964)

(4) Yamamoto, K. and Ishida, M.: J. Nucl. Sci. Technol. 8, 458 (1971)

(5) Stace, R.H.W.: A Review of the use of collision probabilities in lattice calculations (the Bournemouth Symposium on the physics of graphite Moderated Reactors, 1962)

(6) Honeck, H.C.: Nucl. Sci. Engng. 8, 193 (1960)

(7) Nordheim L.W.: (1962) Nucl. Sci. Engng. 12, 457 (1962)
Nordheim L.W., Kuncir G.F.: GA-2527, (1961)

(8) Mizuta, H. et al.: JEARI 1134 (1967)

(9) Komatsu, I. and Fukai, Y.: JEARI 1105 (1966)

(10) Honeck, H.C.: Nucl. Sci. Engng. 18, 49 (1964)

(11) Mizuta, H. and Fukai, Y.: J. Nucl. Energ. 23, 589 (1969)

(12) Honeck, H.C. and Kaplan, I.: Nucl. Sci. Engng. 8, 203 (1960)

(13) PNC-report: SJ 304 70 02-1 2 (1970), SJ 304 70 04-1 2 (1970), SJ 304 69 05-1 2 (1969), see also Part I of this paper

(14) Wajima, J.T. et al.: Internal Report, Hitachi, Ltd., (1968), Mitsui, H., Yamamoto, K., Wajima, J.T. et al.: Trans. ANS Winter Meeting (Washington), (1970)

(15) Takeda, R. and Inoue, K.: J. Nucl. Sci. Technol. 1, 172 (1964)

(16) PNC-report: SJ 302 71-06 (1971)

(17) Shimamura, A. and Kinoshita, M.: to be published

(18) PNC-report: SJ 302 70-05 (1970)

(19) Hellstrand, E.: J. Appl. Phys. 28, 1493 (1957)

(20) Weinberg, A.M. and Wigner, E.: The Physical Theory of Neutron Chain Reactors, The University of Chicago Press, (1958)

(21) Matsuoka, K.: Internal Report, Hitachi, Ltd. (1961)

(22) Yuuki Hachiya and Haruo Hatakenaka: J. Nucl. Sci. Technol. to be published

(23) Yamamoto, K., Kurihara, K. et al.: J Nucl. Sci. Technol. (to be publ

(24) Yamamoto, K., Matsuoka, K., Maesawa, Y.: Preprint 1967 Fall Meeting Reactor Phys. & Reactor Eng., At. Energy Soc. Japan, (1967)

(25) Bollacasa, D., Bonalumi, R.A.: energia nucleare 17, 244 (1970)

(26) Fukai, Y.: Data presented at the Committee of integral transport equation, (1965)

(27) Fukai, Y.: Private communication, (1970)

(28) Amyot, L., Benoist, P.: Nucl. Sci. Eng., 28, 215 (1967)

Appendix

Experimentally, energy is separated at most into two regions: epi-Cd and sub-Cd, corresponding respectively to energies above and below the Cd-cut-off energy. Thus in the present work, the four-factor formula is expressed with the quantities based on the two group scheme, although this treatment obscures somewhat the traditional distinction between fast fission and resonance escape probabilities.

If plutonium exists in the system, then the following parameters must be added as plutonium micro-parameters:

$$\delta^{49'} = \frac{\text{Epi-Cd fission in plutonium}}{\text{Sub-Cd fission in plutonium,}}$$

where 49' means the summation of all isotopes of plutonium, and

$$\delta^{49'}/25 = \frac{\text{Total fission in plutonium}}{\text{Total fission in U235}}$$

(1) Multiplication factor and four factors

$$k_\infty = \varepsilon\, p\, \eta\, f \qquad (A.1)$$

(2) Fast fission factor

$$\varepsilon = 1 + \frac{(\nu\Sigma_f)_1\, \phi_1}{(\nu\Sigma_f)_2\, \phi_2}$$

$$= 1 + \frac{\delta^{25} + (\nu^{28}/\nu^{25})\,\delta^{28}\,(1+\delta^{25}) + (\nu^{49'}/\nu^{25})\,\delta^{49'}\,[F_2^{49'}/F_2^{25}]}{1 + (\nu^{49'}/\nu^{25})\,[F_2^{49'}/F_2^{25}]} \qquad (A.2)$$

where

$$[F_2^{49'}/F_2^{25}] = \delta^{49'/25}\ \frac{1+\delta^{49'}}{1+\delta^{25}} \qquad (A.3)$$

(3) Resonance escape probability

$$P = \frac{\Sigma r}{\Sigma r + \Sigma a1} = \frac{1}{1 + f_{p2}\, R} \qquad (A.4)$$

$$R = \rho^{28}\frac{(1+\alpha_1^{28})^{-1} + (1+\alpha_1^{25})\,\delta^{25}/\rho^{28}\,[F_2^{25}/C_2^{28}] + (1+\alpha_1^{49'})\,\delta^{49'}/\rho^{28}\,[F_2^{49'}/C_2^{28}] + A_1^{\text{nonfuel}}/C_1^{28}}{1 + (1+\alpha_2^{25})\,[F_2^{25}/C_2^{28}] + (1+\alpha_2^{49'})\,[F_2^{49'}/C_2^{28}]} \qquad (A.5)$$

where

$$[F_2^{25}/C_2^{28}] = \frac{1+\rho^{28}}{1+\delta^{25}} \cdot \frac{1}{CR} \qquad (A.6)$$

$$[F_2^{49}/C_2^{28}] = \frac{1+\rho^{28}}{1+\delta^{49}} \cdot \frac{\delta^{49}/_{25}}{CR} \qquad (A.7)$$

Here, CR is the conversion ratio (total capture rate of U^{238} to total fission rate of U^{235}, P_2 the non escape probability of sub-Cd-neutrons, and α the capture-to-fission ratio.

(4) Thermal utilization factor and η

$$f^{-1} = 1 + \sum_{i \neq f} \frac{V_i \Sigma_{a2}^i}{V_{fuel} \Sigma_{a2}^{fuel}} (\sigma_{Dy}^{fuel}/\sigma_{Dy}^i) [DF_i(Dy)] \qquad (A.8)$$

$$\eta = \overline{(\nu \Sigma_f)}_2 / \Sigma_{a2}^{fuel}$$

The calculated value is generally used for η.